Image segmentation of micro-TIG battery welds

Carlo Ferri*, Malarvizhi Kaniappan Chinnathai†, Rohin Titmarsh ‡ and Hala Abdelaziz§

* ‡ § WMG, The University of Warwick

6 Lord Bhattacharyya Way, Coventry, CV4 7AL, UK

* ORCID: 0000-0002-2362-0312

Email: * c.ferri@warwick.ac.uk, ‡ rohin.titmarsh@warwick.ac.uk, § hala.abdelaziz@warwick.ac.uk

† Brunel Innovation Centre, Brunel University

TWI, Granta park, Great Abington, Cambridge, CB21 6AL, UK

Email: m.kaniappan-chinnathai.2@warwick.ac.uk

Abstract

Inspection of cell-to-tab welds in module assembly for battery pack is one the most critical processes in the production of battery packs for transportation electrification. A procedure suitable for the segmentation of weld images on module assembly lines is proposed to separate them into weld and tab regions. The procedure is centred around identifying the edge of the weld and the convex hull region that includes it. The edge is detected with a fuzzy logic rule-based inference system. The procedure is demonstrated with a set of 71 images that are labelled to establish a comparison reference, the so called ground truth. Particle swarm optimisation is used to find values of the parameter procedure that result in a a local minimum of the mean percent error (MPE). An MPE of 4.25 per cent has been obtained.

Index Terms

transportation electrification, fuzzy logic, particle swarm optimisation

I. Introduction

A number of segmentation approaches have been proposed in the detection of weld defects in radiographic images. Among these approaches, Malarvel *et al.* [1] proposed an improved Otsu's method that automatically selects the threshold value using the Weibull distribution. Rathod and Anand [2] compared three segmentation methods: the edge- and boundary-based method, the region-growing method and the watershed transformation method. Mahmoudi and Regragui [3] developed a segmentation approach based on contrast enhancement, histogram analysis, global image thresholding using the Otsu's method and local image thresholding using the Sauvola method. Carrasco and Mery [4] presented a weld defect detection method that comprises edge detection, binary thresholding and the application of watershed transform.

In welding robotic systems, vision sensors have been used to track the weld seam. Haldankar *et al.* [5] have reviewed software architectures and methods for weld images in real-time seam tracking, including segmentation.

NON-SLIP project, grant number 8232, HVM Catapult, WMG, The University of Warwick, UK.

For gas metal arc welding (GMAW), Xu *et al*. [6] proposed a method for identifying the weld seam in real-time using the Otsu's method and edge detection filters.

Sun and Li [7], in surveying meta-learning algorithms for image segmentation, have highlighted the challenge of applying segmentation methods based on deep learning in those applications where a large amount of labelled data is unavailable. Sultana *et al.* [8] have surveyed the evolution and the state-of-the-art of image segmentation methods using deep convolutional neural networks.

In prototype and small-series production of battery packs for transportation electrification and special applications, Micro-TIG welding is often used for joining cells to tabs. In this production scenario, labelled images in large amount are often hardly available.

Moreover, the image characteristics of the joints may vary significantly from a small series to another. For example, a batch may have copper tabs, which are red-orange in colour, another nickel-coated tabs, which are grey. Therefore a segmentation method should adapt easily to variations between batches to be of greater practical use.

Segmentation methods of weld images specifically designed for the automatic micro-TIG welding of cells to tabs in small-series production have not been found in the literature. In the detection of blood vessels in retinal fundus images, Orujov *et al.* [9] demonstrated the flexibility of fuzzy logic edge detection by evaluating the universal method that they have proposed on three different image datasets. They have also showed that the accuracy of their method is significantly better than the performance of the classical methods for boundary detection specifically developed for each of the three datasets. Classical methods that they considered for comparison were the Laplacian, the Robert, the Robinson, the Scharr, and the Sobel methods.

An approach to micro-TIG image segmentation based on fuzzy logic edge detection and particle swarm optimisation (PSO) is proposed in this paper.

In Section II the proposed segmentation method is introduced. In Section III, the particle swarm optimisation variables and the fuzzy edge detection parts of the segmentation method are defined. In Section IV, numerical results are presented. Conclusions are then drawn in Section V.

II. Segmentation

The proposed segmentation procedure consists of the steps in the subsections that follows and that are described using the symbols and the conventions for system flowcharts prescribed by the ISO 5807:1985 [10].The system flowchart is shown in Fig. 1.

A. Taking weld colour images

A set of colour images of micro-TIG welds made in stable process conditions is formed. The number of images is sufficiently large to make the set representative of the whole future weld production in the same stable conditions.

B. Image downscaling

The images are scaled down to a number of pixels that makes the processing time compatible with the short cycle time of battery module assembly. The aspect ratio of the original images is preserved. The parameters of this image resizing are not part of any optimisation.

C. Pixel labelling

The pixels of the downscaled images are labelled as weld and tab. they are marked as one and zero, respectively. The tab pixels constitute the background, the weld pixels constitute the foreground or region of interest. A mask set, i.e. a set binary images, is the output of the labelling process and is designated with GT. The pixels labelled as weld are the ground truth. The meaning of the expression *ground truth* used here is 'information obtained by direct visual examination, esp. as used to check or calibrate an automated recognition system' [11]. Pixel labelling is therefore performed by a person using interactive software tools. Examples of these tools have been surveyed by Sagar *et al.* [12].

D. Converting images to grayscale

Each colour image is separated into its three colour components in the RGB (red, green, blue) and in the HSV (hue, saturation, value) colour spaces. Each colour image is also converted to grayscale by eliminating the hue and the saturation while retaining the luminance. The grayscale pixel value is obtained by the following weighted sum of the red, green and blue components:

$$E'y = 0.2989E'_R + 0.5870E'_G + 0.1140E'_B \tag{1}$$

The weights in (1) rounded to three decimals are the same as those used to calculate the luminance $E'y$ in the recommendation ITU-R BT.601-7 ([13], page 4). In this way, seven grayscale image sets are obtained and designated as G_i with $i = 1, \ldots, \mathrm{N}$ and $\mathrm{N} = 7$. The procedure is run separately on each of the seven grayscale image sets obtained.

E. Particle swarm core fuzzy procedure

A software procedure based on the detection of edges and the computation of their convex hulls returns a set of masks designated as C_i. Each set C_i corresponds to the input grayscale images in the set G_i. As in the ground truth mask set, weld pixels are marked with one and tab pixels with zero.

F. Computing the MPE_i

The per cent error between the computed mask and the ground truth is calculated for each mask in the output from the core procedure, C_i, and the corresponding mask in the ground truth set, GT. The mean per-cent error over the computed mask set C_i is then calculated and designated as MPE_i.

As a part of the core procedure, a population of values for the vector of optimisation variables is generated randomly in the domain of the function under optimisation. The population is referred to as a swarm. Each vector in the swarm is called a *particle*, although the creators of the algorithm also discuss the term *point*, before excluding it [14]. For each particle in the swarm the mean per-cent error, i.e. the MPE, is then calculated. The particle yielding the minimum MPE is selected as the candidate local optimum. Together with the swarm, a vector of particle change is also calculated for each particle. The vector of changes is called *velocity* vector. The availability of a velocity vector allows an iterative process to take place: the velocity vector is added to the initial swarm of particles so that a second swarm of particles is obtained. As the names suggest, the second particle swarm can also be seen as a displacement of the first swarm during a dimension-less time step, i.e. during an iteration. The generation of new swarms continues until a stopping criterion is met. In the proposed

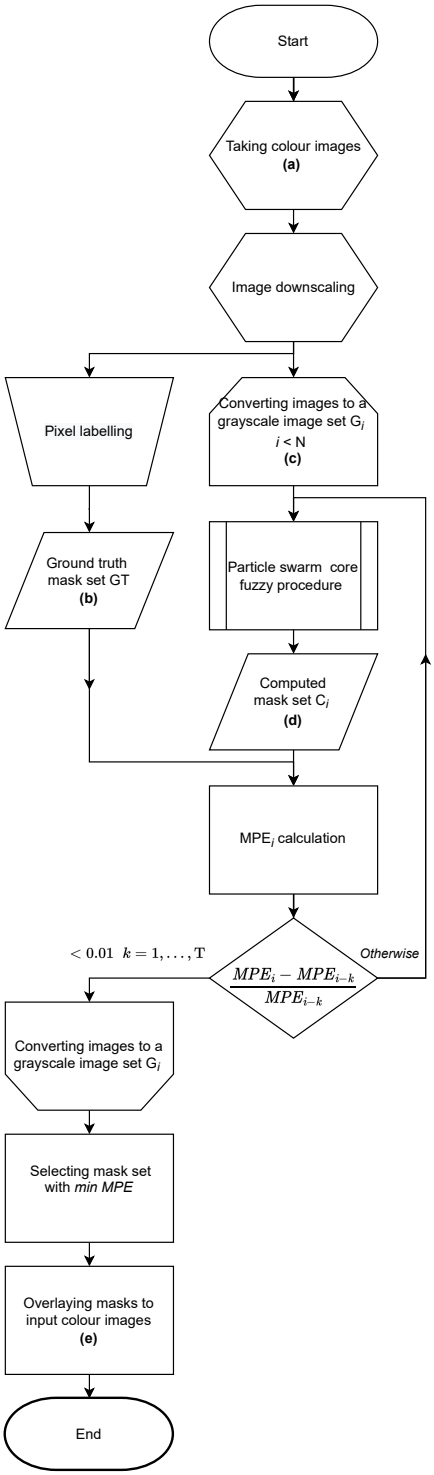

Fig. 1. System flowchart of the proposed procedure.

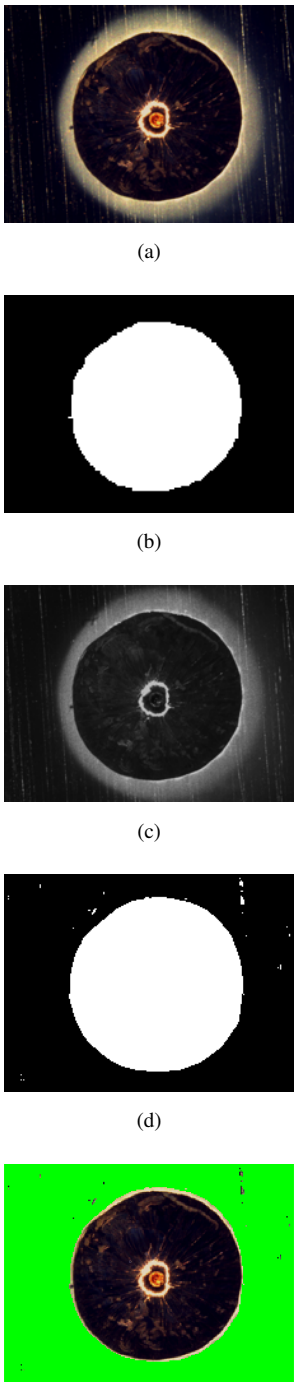

Fig. 2. (a) A weld colour image. (b) A ground truth mask. (c) Grayscale image in the blue set. (d) Computed locally-optimal mask. (e) Locally-optimal weld segment.

procedure the stopping criterion consists in obtaining a proposed local minimum MPE that has not changed more than $\mathrm{P}\,\%$ in the last T iterations.

G. Selecting the locally-optimal mask set

The set of computed masks C_i that yields the minimum per cent error over the seven grayscale image sets G_i is selected.

H. Overlaying the masks to the input colour images

Each mask in the locally optimal mask set found is overlaid to each of the RGB or HSV components of the colour images in the downscaled colour image set. The weld colour segments are therefore obtained. Overlaying occurs by element-wise multiplication, a.k.a. Shur product.

III. Particle swarm core fuzzy procedure

The particle swarm core procedure consists of a sequence of processes described in the subsections that follow and illustrated with a flowchart in Fig. 3.

A. Setting values to optimisation variables

The variables whose values is tuned to determine a local minimum for the MPE are as it follows:

- X_1: The standard deviation of the Gaussian kernel used to filter each grayscale image set.
- X_2: The standard deviation of the Gaussian membership function defining the fuzzy set `zero_H` for the horizontal gradient in the grayscale images.
- X_3: The standard deviation of the Gaussian membership function defining the the fuzzy set `zero_V` for the vertical gradient in the grayscale images.
- X_4: The value identifying the beginning of the triangular membership function defining the fuzzy set `edge` having the other two vertices in $(1, 0)$ and $(1, 1)$.

The standard deviation X_1 is further described in Section III-B. The remaining three variables X_2, X_3, X_4 are a part of the edge detection procedure based on fuzzy logic and described in Section III-C.

B. Image filtering

Each image in the set G_i is filtered with a Gaussian filter, whose standard deviation in pixels, X_1, is the first variable considered in the minimisation of the MPE. A square filter kernel is used, whose side length in pixels, *fs*, is set as a function of the standard deviation as displayed in (2), where the symbol $\lceil X \rceil$ represents the smallest positive integer greater than x.

$$fs = 2\lceil 2X_1 \rceil + 1 \tag{2}$$

When convolving an image with the filter kernel, any needed padding at the image border is performed by repeating the border pixels.

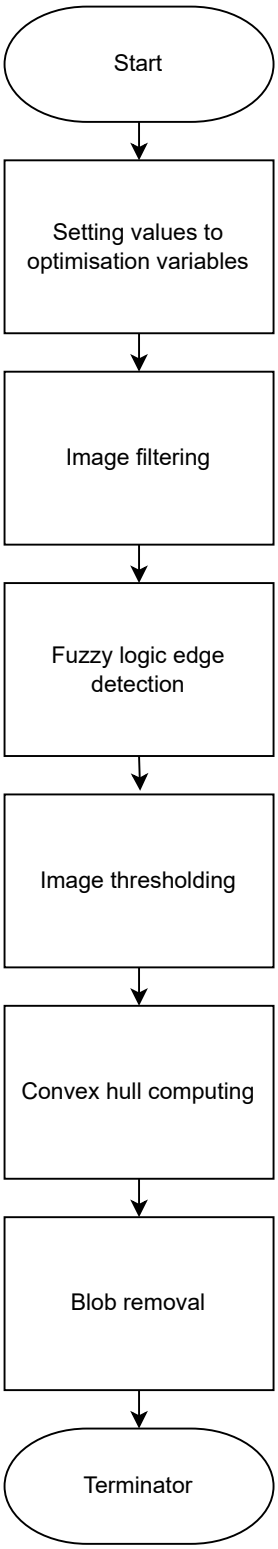

Fig. 3. Flowchart of the particle swarm core fuzzy procedure.

C. Fuzzy logic edge detection

The edges of the weld segment in each filtered image in input to this step are detected by a rule-based fuzzy inference system (FIS). First, the gradients of the pixel luminance in the horizontal and in the vertical directions are calculated. The following two rules, **R1** and **R1**, are then used to compute the degree of membership of each input image pixel:

R1: If `horizontal_gradient` is `zero_H` and `vertical_gradient` is `zero_V` then `FIS_output_pixel` is not `edge`.

R2: If `horizontal_gradient` is not `zero_H` or `vertical_gradient` is not `zero_V` then `FIS_output_pixel` is `edge`.

The labels `horizontal_gradient` and `vertical_gradient` represent the two universes of discourse on which the two fuzzy sets `zero_H` and `zero_V` are defined. The meaning of the expression *universe of discourse* is taken from the Oxford English Dictionary as 'all those objects, elements, etc., that the terms of a proposition may refer to; a universal set; the totality of things under consideration' [15]. The fuzzy sets `zero_H` and `zero_V` have a suffix in their designation just to distinguish the universe of discourse to which each of them refers to. The label `zero_H` indicates the class of horizontal gradient values close enough to zero to be considered indistinguishable from it. The label `zero_V` indicates the same for the vertical gradient. The vagueness in the definition of these two classes is conveniently described with 'a continuum of grades of membership' [16]. Gaussian membership functions centred around zero and with standard deviation X_2 and X_3 are used to represent the grade of membership to `zero_H` and `zero_V`, respectively. The expression of these two functions is in (3).

$$\mu_{\mathrm{zero\_}_j}(x) = \exp\left(-\frac{x^2}{2{X_k}^2}\right) \;\; j = \mathrm{H}, \mathrm{V}; \;\; k = 2, 3 \tag{3}$$

where the symbol $\mu_{\mathrm{zero\_}_j}(x)$ indicates the grade of membership of the gradient value x to the set $\mathrm{zero\_}_j$ with $j = \mathrm{H}, \mathrm{V}$. The subscript k equals two if $j = H$ and equals three if $j = V$. The label `FIS_output_pixel` represents the universe of discourse on which the fuzzy set `edge` is defined. This universe is constituted by the real numbers in the interval $[0, 1]$. The triangular membership function in (4) and (5) characterised by the parameter X_4 is used to model the `edge` fuzzy set.

$$\mu_{\mathrm{edge}}(x) = 0 \;\; if \;\; x \leq \; X_4; \tag{4}$$

$$\mu_{\mathrm{edge}}(x) = \frac{x - X_4}{1 - X_4} \;\; if \;\; x > \; X_4; \tag{5}$$

The triangular membership function is displayed in Fig. 4.

The evaluation of the two rules in the FIS allows the computation of the degree of membership to the fuzzy set `edge`. Every pixel in each image in output to the FIS is initially assigned a zero value. As a result of the FIS evaluation, this computed degree of membership is given as a value to the pixels in the output images. Therefore a pixel value one, i.e. a white pixel, describes an edge known with high confidence, a zero, i.e. a black pixel, describes an image part that is not an edge with equally high confidence. All the grayscale values in between express the level of confidence that the pixel in question may be an edge.

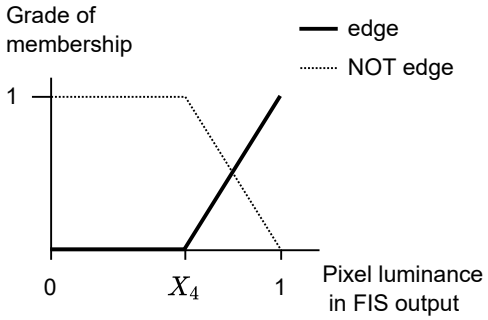

Fig. 4. The triangular membership functions identifying the fuzzy sets `edge` and its complement fuzzy set `NOT edge` in the universe of discourse `FIS_output_pixel`.

D. Image thresholding

The grayscale image set in output from the edge detection process is transformed to a binary zero-one image set by the Otsu's method. This method selects the threshold value to minimize the intraclass variance of the thresholded black and white pixels. By thresholding, the uncertainty about the attribution of pixels to the edge class or the not-edge class is eliminated.

E. Convex hull computing

For each set of white pixels describing an edge a convex hull is calculated. Each convex hull is marked with white pixels. This process makes it possible to identify those areas of the images that are inside an edge as weld regions.

F. Blob removal

Some of the pixel groups identified by computing convex hulls are too small to have any practical importance in the welding process. Those convex hulls made of less than an empirically-established number of pixels are set to zero. For the image set considered, the lower limit for the pixel number was set to 150 pixels.

IV. RESULTS

The Particle swarm core fuzzy procedure and the MPE_i calculation in Fig. 1 have been implemented in a program using MATLAB and the MATLAB Parallel Computing Toolbox. The program has been run separately for each grayscale image set G_i on a Unix-type high performance computer system (HPC) with 800 cores, of which 91 were used in a parallel cluster to execute the program.

In the stopping criterion described in Section II-F, the parameters $\mathrm{P}\,\%$ and T have been set to 1 % and 20 iterations, respectively. This choice has made it possible for the program execution on each of the seven G_i image datasets to terminate always within the maximum number of iterations set to 800, when the number of particles in each iteration is set to 200. That is, with the swarm size set to 200, the program executions have always terminated within 800 swarm generations.

In Tab. I the local minimum MPE_i values for each of the considered image sets G_i is displayed. The blue image set yields the smallest MPE_i value. The corresponding computed mask set is selected. The actual

TABLE I
NUMERICAL RESULTS

G_i	MPE_i	Iteration count	Evaluation count	Run time, second /s
Red	4.96	33	6800	2442
Green	4.42	35	7200	2659
Blue	4.25	36	7400	2346
Hue	9.66	40	8200	2685
Saturation	30.0	23	4800	1899
Value	4.95	38	7800	2550
Grayscale	4.69	35	7200	2553

number of iterations with a swarm size of 200, the number of MPE_i evaluations and the program run time on the above-described system are also displayed.

The actual number of iterations in In Tab. I is far below the maximum number of iterations that has been set: increasing this maximum does not change the MPE_i. The values of the parameters $\mathrm{P}\,\%$ and T have been set specifically to obtain this effect. Further MPE_i reductions might be obtained by increasing the swarm size at the cost of an increased run time. Quantifying these potential reductions is beyond the purpose of this investigation.

V. CONCLUSIONS

A procedure for segmenting colour images of micro-TIG welds is proposed. The procedure aims to be part of weld inspection processes in battery module assembly lines. Fuzzy logic edge detection complemented by the determination of their convex hull appears a viable strategy for the stated aim. A demonstration of the implemented software programs on a set of 71 micro-TIG labelled images resulted in a local minimum per cent error of 4.25.

ACKNOWLEDGMENT

This investigation was performed as part of the research project NON-SLIP, *Machine Learning for On-line Cell-to-busbar Weld Visual Inspection*, funded by the UK program High Value Manufacturing Catapult at WMG, The University of Warwick.

REFERENCES

[1] M. Malarvel, G. Sethumadhavan, P. C. R. Bhagi, S. Kar, and S. Thangavel, "An improved version of otsu's method for segmentation of weld defects on x-radiography images," *Optik*, vol. 142, pp. 109–118, 2017. [Online]. Available: https://www.sciencedirect.com/science/article/pii/S0030402617306022

[2] V. R. Rathod and R. Anand, "A comparative study of different segmentation techniques for detection of flaws in nde weld images," *Journal of Nondestructive Evaluation*, vol. 31, no. 1, pp. 1–16, 2012.

[3] A. Mahmoudi and F. Regragui, "Welding defect detection by segmentation of radiographic images," in *2009 WRI World Congress on Computer Science and Information Engineering*, vol. 7. IEEE, 2009, pp. 111–115.

[4] M. Carrasco and D. Mery, "Segmentation of welding defects using a robust algorithm," *Materials Evaluation*, vol. 62, no. 11, pp. 1142–1147, 2004.

[5] T. Haldankar, S. Kedia, R. Panchmatia, D. Parmar, and D. Sawant, "Review of implementation of vision systems in robotic welding," in *2021 5th International Conference on Intelligent Computing and Control Systems (ICICCS)*, 2021, pp. 692–700.

[6] Y. Xu, G. Fang, S. Chen, J. J. Zou, and Z. Ye, "Real-time image processing for vision-based weld seam tracking in robotic gmaw," *The international journal of advanced manufacturing technology*, vol. 73, no. 9-12, pp. 1413–1425, 2014.

[7] J. Sun and Y. Li, "Metaseg: A survey of meta-learning for image segmentation," *Cognitive Robotics*, vol. 1, pp. 83–91, 2021. [Online]. Available: https://www.sciencedirect.com/science/article/pii/S2667241321000070

[8] F. Sultana, A. Sufian, and P. Dutta, "Evolution of image segmentation using deep convolutional neural network: A survey," *Knowledge-Based Systems*, vol. 201-202, p. 106062, 2020. [Online]. Available: https://www.sciencedirect.com/science/article/pii/S0950705120303464

[9] F. Orujov, R. Maskeliūnas, R. Damaševičius, and W. Wei, "Fuzzy based image edge detection algorithm for blood vessel detection in retinal images," *Applied Soft Computing*, vol. 94, p. 106452, 2020. [Online]. Available: https://www.sciencedirect.com/science/article/pii/S1568494620303926

[10] *Specification for Data processing flow chart symbols, rules and conventions — [ISO title: Information processing — Documentation symbols and conventions for data, program and system flowcharts, program network charts and system resources charts]*, BSI Std. BS 4058:1987 ISO 5807-1985, ISBN 0 580 15271.

[11] Oxford English Dictionary. ground truth, n. Accessed on 2 February 2022. [Online]. Available: https://www.oed.com/view/Entry/249130

[12] C. Sager, C. Janiesch, and P. Zschech, "A survey of image labelling for computer vision applications," *Journal of Business Analytics*, vol. 4, no. 2, pp. 91–110, 2021. [Online]. Available: https://doi.org/10.1080/2573234X.2021.1908861

[13] T. I. R. Assembly, "Recommendation ITU-R BT.601-7 (03/2011) studio encoding parameters of digital television for standard 4:3 and wide-screen 16:9 aspect ratios," International Telecommunication Union (ITU), Place des Nations, 1211 Geneva 20 Switzerland, Tech. Rep. ITU-R BT.601-7, 2017.

[14] J. Kennedy and R. Eberhart, "Particle swarm optimization," in *Proceedings of ICNN'95 - International Conference on Neural Networks*, vol. 4, 1995, pp. 1942–1948 vol.4.

[15] Oxford English Dictionary. universe, n. Accessed on 5 February 2022. [Online]. Available: https://www.oed.com/view/Entry/214800?redirectedFrom=universe+of+discourse

[16] L. Zadeh, "Fuzzy sets," *Information and Control*, vol. 8, no. 3, pp. 338–353, 1965. [Online]. Available: https://www.sciencedirect.com/science/article/pii/S001999586590241X